Hindawi Publishing Corporation
Journal of Chemistry
Volume 2016, Article ID 5129010, 12 pages
http://dx.doi.org/10.1155/2016/5129010

Research Article

Synthesis, Biological, and Quantum Chemical Studies of Zn(II) and Ni(II) Mixed-Ligand Complexes Derived from N,N-Disubstituted Dithiocarbamate and Benzoic Acid

Anthony C. Ekennia,[1] Damian C. Onwudiwe,[2,3] Aderoju A. Osowole,[4] Lukman O. Olasunkanmi,[2,3,5] and Eno E. Ebenso[2,3]

[1]*Department of Chemistry, Federal University Ndufu-Alike Ikwo (FUNAI), PMB 1010, Abakaliki, Ebonyi, Nigeria*
[2]*Material Science Innovation and Modelling (MaSIM) Research Focus Area, Faculty of Agriculture, Science and Technology, North-West University, Mafikeng Campus, Private Bag Box X2046, Mmabatho 2735, South Africa*
[3]*Department of Chemistry, School of Mathematical and Physical Sciences, Faculty of Agriculture, Science and Technology, North-West University, Mafikeng Campus, Private Bag Box X2046, Mmabatho 2735, South Africa*
[4]*Inorganic Unit, Department of Chemistry, University of Ibadan, Oyo State, Nigeria*
[5]*Department of Chemistry, Faculty of Science, Obafemi Awolowo University, Ife 220005, Nigeria*

Correspondence should be addressed to Damian C. Onwudiwe; Damian.Onwudiwe@nwu.ac.za
and Eno E. Ebenso; eno.ebenso@nwu.ac.za

Received 22 January 2016; Revised 29 February 2016; Accepted 1 March 2016

Academic Editor: Josefina Pons

Some mixed-ligand complexes of Zn(II) and Ni(II) derived from the sodium salt of *N*-alkyl-*N*-phenyl dithiocarbamate and benzoic acid have been prepared. The complexes are represented as ZnMDBz, ZnEDBz, NiMDBz, and NiEDBz (MD: *N*-methyl-*N*-phenyl dithiocarbamate, ED: *N*-ethyl-*N*-phenyl dithiocarbamate, and Bz: benzoate); and their coordination behavior was characterized on the basis of elemental analyses, IR, electronic spectra, magnetic and conductivity measurements, and quantum chemical calculations. The magnetic moment measurement and electronic spectra were in agreement with the four proposed coordinate geometries for nickel and zinc complexes and were corroborated by the theoretical quantum chemical calculations. The quantum chemically derived thermodynamics parameters revealed that the formation of *N*-methyl-*N*-phenyl dithiocarbamate complexes is more thermodynamically favourable than that of the *N*-ethyl-*N*-phenyl dithiocarbamate complexes. The bioefficacy of the mixed-ligand complexes examined against different microbes showed moderate to high activity against the test microbes. The anti-inflammatory and antioxidant studies of the metal complexes showed that the ethyl substituted dithiocarbamate complexes exhibited better anti-inflammatory and antioxidant properties than the methyl substituted dithiocarbamate complexes.

1. Introduction

The chemistry of transition metal complexes with mixed ligands is an area of current interest due to their structural diversity and usefulness. They have been reported to possess properties such as electrical conductivity [1], nonlinear optical applications [2], and antimicrobial activities [3, 4]. Mixed-ligand complexes have a unique role in biological chemistry because they mimic biological molecules as millions of potential ligands are likely to compete for metal ions *in vivo* [5].

Inflammation is recognized as a defensive response by the body's vascular tissue to different external inflammatory stimuli, in which the body induces physiological adaptation to minimize tissue damage and to remove the extraneous variable [6]. Most often, inflammation is characterized by series of cellular and modular events including dilation of arterioles, venules, and capillaries with increased vascular permeability, exudation of fluids containing plasma proteins, and migration of leukocytes into the inflammatory area [7]. Diseases like rheumatism, encephalitis, pneumonia, oesophagitis, cancer, protein denaturation, heart problem,

and fibrosis have been implicated in chronic inflammation [6]. It has been observed that patients with rheumatic diseases and rats with inflammatory lesions experience albumin denaturation. Protein (albumin) denaturation is a process in which proteins lose their structures as a consequence of the application of external stress and as a result it leads to chronic inflammation [8]. Nonsteroidal anti-inflammatory drugs (NSAIDs) and opioid analgesics like salicylic acid, phenylbutazone, and so forth have been studied for their potentials to inhibit albumin denaturation and were reported to possess dose dependent ability to inhibit thermally induced albumin denaturation [9]. However, the main side effect of most NSAIDs is gastric ulceration [10, 11]. Hence, there is a need to discover novel inhibitors against albumin denaturation and reactive oxygen species (ROS) capable of causing inflammation.

Various synthesized zinc and nickel dithiocarbamate based compounds have been reported as potent antibacterial, antifungal, and anticancer drugs and also as imaging agents [12–14]. However, there is scarce information on the antioxidant and protein denaturation inhibitory properties of these compounds. Hence, we report herein the synthesis, characterization, and biological (antimicrobial, anti-inflammatory, and antioxidant) evaluation of some novel zinc(II) and nickel(II) mixed-ligand complexes containing dithiocarbamate and benzoate. Furthermore, we studied the effect of different substituents of the dithiocarbamate on the overall biological properties of the complexes. Quantum chemical calculations were also carried out *in vacuo*, using the density functional theory (DFT) method to ascertain the geometry of the complexes and their electronic properties.

2. Experimental Section

2.1. Materials. Nickel(II) chloride hexahydrate, zinc(II) sulphate heptahydrate, carbon disulfide, bovine serum albumin, $FeSO_4{\cdot}7H_2O$, 2,2-diphenyl-1-picrylhydrazyl (DPPH), phosphate buffer, 1,10-phenanthroline, benzoic acid, *N*-ethyl aniline, and *N*-methyl aniline (Aldrich) were used as received. Reagent grade methanol, DMSO, and diethyl ether (Ace Chemicals) were used directly.

2.2. Physical Measurements. The percentages of C, H, N, and S were determined by Elementar, Vario EL Cube, set up for CHNS analysis (InnoVenton, NMMU). UV-Vis spectra were obtained on a Perkin Elmer Lambda 40 UV-Vis spectrophotometer. FTIR spectra were recorded in the range of 4000–400 cm^{-1} on a Bruker alpha-P FTIR spectrophotometer. Magnetic susceptibilities were measured on a Johnson Matthey magnetic susceptibility balance and diamagnetic corrections were calculated using Pascal's constant. Conductivity measurements were conducted using MC-1, Mark V conductivity meter with a cell constant of 1.0.

2.2.1. Preparation of the Ligands: N-Methyl-N-phenyl Dithiocarbamate and N-Ethyl-N-phenyl Dithiocarbamate. Sodium *N*-methyl-*N*-phenyl dithiocarbamate, NaMD, and sodium *N*-ethyl-*N*-phenyl dithiocarbamate, NaED, were synthesized according to the published procedure [15].

2.2.2. Preparation of Zn(II) and Ni(II) Complexes with N-Methyl-N-phenyl Dithiocarbamate and Benzoic Acid. Sodium *N*-methyl-*N*-phenyl dithiocarbamate, NaMD, was synthesized according to the published procedure [15]. The ligand, NaMD (0.50 g, 2.4 mmol), in ethanol (10 mL) was mixed with a solution of benzoic acid (0.29 g, 2.4 mmol) in 5 mL ethanol and stirred for 5 min. To the resultant mixture, 5 mL ethanol solution of 2.4 mmol was added ($ZnSO_4{\cdot}7H_2O$ and $NiCl_2{\cdot}6H_2O$) and stirred at room temperature for 3 h. The precipitate obtained was filtered and stored under vacuum.

NiMDBz: (Yield 0.35 g, 70%). Elemental analysis for $[NiC_{15}H_{13}NS_2O_2]{\cdot}H_2O$ (380.12): C, 47.40; H, 3.99; N, 3.57; S, 16.72. Found: C, 47.39; H, 3.97; N, 3.68; S, 16.87. FTIR: ν/cm^{-1}: 3530b, 3004m, 2903m, 2895m, 1556s, 1534s, 1478s, 1462s, 1272m, 1268m, 910s, 902m, 465m. UV-Vis: 15380, 24040, and 41150 cm^{-1}. Magnetic moment: Zero; Conductance ($\Omega^{-1}cm^2mol^{-1}$): 19.9.

ZnMDBz: (Yield 0.42 g, 82%). Elemental analysis for $[ZnC_{15}H_{13}NS_2O_2]{\cdot}2H_2O$ (404.81): C, 44.29; H, 4.53; N, 3.38; S, 15.80. Found: C, 44.50; H, 4.23; N, 3.46; S, 15.84. FTIR: ν/cm^{-1}: 3478b, 3007m, 2900m, 2792m, 1578s, 1552s, 1483s, 1461s, 1275m, 1262m, 917s, 901m, 462m. UV-Vis: 24940, 29330, and 46950 cm^{-1}. Magnetic moment: Zero; Conductance ($\Omega^{-1}cm^2mol^{-1}$): 8.53.

2.2.3. Preparation of Zn(II) and Ni(II) Complexes with N-Ethyl-N-phenyl Dithiocarbamate and Benzoic Acid. The ligand, NaED (0.5 g, 2.3 mmol), was dissolved in ethanol (10 mL) and mixed with a solution of benzoic acid (0.28 g, 2.3 mmol) in 5 mL of ethanol. The mixture was stirred for 5 min. To the resultant solution, 5 mL of ethanol solution of 2.3 mmol was added ($ZnSO_4{\cdot}7H_2O$ and $NiCl_2{\cdot}6H_2O$) and stirred at room temperature for 3 h. The precipitate obtained was filtered and stored under vacuum.

NiEDBz: (Yield 0.32 g, 64%). Elemental analysis for $[NiC_{16}H_{15}NS_2O_2]{\cdot}2H_2O$ (412.15): C, 46.63; H, 4.65; N, 3.40; S, 15.56. Found: C, 46.58; H, 4.56; N, 3.21; S, 15.50. FTIR: ν/cm^{-1}: 3537b, 3023m, 2933m, 2858m, 1579s, 1521s, 1465s, 1459s, 1287m, 1265m, 917s, 901m, 462m. UV-Vis: 11590, 15060, 25130, 29240, and 40320 cm^{-1}. Magnetic moment: Zero; Conductance ($\Omega^{-1}cm^2mol^{-1}$): 6.84.

ZnEDBz: (Yield: 0.42 g, 82%). Elemental analysis for $[ZnC_{16}H_{15}NS_2O_2]{\cdot}2H_2O$ (418.84): C, 45.88; H, 4.57; N, 3.34; S, 15.31. Found: C, 45.78; H, 4.52; N, 3.30; S, 15.53. FTIR: ν/cm^{-1}: 3501b, 3010m, 2937m, 1560s, 1529s, 1470s, 1458s, 1270m, 1263m, 923s, 899m, 449m. UV-Vis: 24960, 28650, and 32790 cm^{-1}. Magnetic moment: Zero; Conductance ($\Omega^{-1}cm^2mol^{-1}$): 5.16.

2.3. Computational Details. Quantum chemical calculations were carried out on the ligands (NaMD, NaED, and Bz) and their metal complexes (NiMDBz, NiEDBz, ZnMDBz, and ZnEDBz) *in vacuo*, using the density functional theory (DFT) method involving the Becke 3-parameter exchange

functional together with the Lee-Yang-Parr correlation functional (B3LYP) [16, 17]. The B3LYP has been successfully used in some previous works for geometry optimization of transition metal complexes [18–21]. It has proven sufficient to produce acceptable geometry and spectroscopic parameters comparable to experimental crystallographic data for some transition metal complexes at moderate computational cost [20].

The 6-31+G(d,p) basis set was used for C, H, N, O, and S atoms, while the metal ions were described by the LANL2DZ relativistic pseudopotential. The LANL2DZ relativistic pseudopotential has been found to be reliable for quantum chemical studies on transition metal complexes [19, 22–27]. It is a "double" quality basis set which uses the Duning D95 V basis set on the first row atoms and Los Alamos ECP plus DZ on Na-Bi [21, 28–31]. It is computationally efficient and suitable for a variety of transition metal complexes [21, 32–34]. The placement of the ECP on transition metal ions via the use of the LANL2DZ basis set has been reported to yield results at similar level of accuracy to the all-electron basis set, such as DZVP [24, 35]. DFT computational model similar to the one used in the present work has been previously employed by Gorelsky et al. [20] for theoretical description of some metal complexes of sulphur containing chelating resin [20]. All the ligands and metal complexes were modeled with GaussView 5.0 software. Gas phase geometry optimizations were carried out without symmetry constraint by using the Gaussian 09W D.01 software [36]. Force constant and vibrational frequency calculations were also performed on all the molecules. The optimized structures were confirmed to correspond to their respective ground state energy minima with the absence of imaginary frequency in the calculated vibrational spectra.

Geometry, electronic, and thermodynamic parameters were obtained from the optimized geometries. The frontier molecular orbital energies, the energies of the highest occupied and the lowest unoccupied molecular orbitals (E_{HOMO} and E_{LUMO}, resp.), and the energy gap ($\Delta E = E_{\mathrm{LUMO}} - E_{\mathrm{HOMO}}$) were calculated. The ionization potential, I ($I = -E_{\mathrm{HOMO}}$), and electron affinity, A ($A = -E_{\mathrm{LUMO}}$), are related to the electronegativity, χ, and global hardness, η, as

$$\chi = \frac{1}{2}(I + A)$$
$$\eta = \frac{1}{2}(I - A). \quad (1)$$

The binding energy, BE, was calculated for each of the metal complexes as the energy required to disassemble the metal complex into its constituent ligands and metal ion, equivalent to the energy difference for the reaction equation shown in Scheme 1.

According to Scheme 1, BE was calculated as

$$\mathrm{BE} = E_{(\text{M-complex})} - \left(E_{(\mathrm{MD/ED})} + E_{(\mathrm{Bz})} + E_{(\mathrm{M^{2+}})}\right), \quad (2)$$

where $E_{(\text{M-complex})}$, $E_{(\mathrm{MD/ED})}$, $E_{(\mathrm{Bz})}$, and $E_{(\mathrm{M^{2+}})}$ are the energies of the metal complex, the ligands (MD or ED), Bz, and the metal ion (M^{2+}), respectively. Other thermodynamic parameters such as the change in enthalpy (ΔH), entropy (ΔS), and Gibb's free energy (ΔG) of complexation were calculated according to

$$\Delta H = H_{(\text{M-complex})} - \left[H_{(\mathrm{MD/ED})} + H_{(\mathrm{Bz})} + H_{(\mathrm{M^{2+}})}\right]$$
$$\Delta S = S_{(\text{M-complex})} - \left[S_{(\mathrm{MD/ED})} + S_{(\mathrm{Bz})} + S_{(\mathrm{M^{2+}})}\right] \quad (3)$$
$$\Delta G = G_{(\text{M-complex})} - \left[G_{(\mathrm{MD/ED})} + G_{(\mathrm{Bz})} + G_{(\mathrm{M^{2+}})}\right],$$

where H_i, S_i, and G_i are the enthalpy, entropy, and free energy of, respectively, the corresponding species i in Scheme 1.

2.4. Biological Studies

2.4.1. Antibacterial Assay (Agar Diffusion Method). The assay was carried out on the ligand and its metal(II) complexes *in vitro* using the agar diffusion method [37]. The bacteria used were identified laboratory strains of Gram negative bacteria (*K. oxytoca, P. aeruginosa*, and *E. coli*) and Gram positive bacteria (*B. cereus* and *S. aureus*). The bacteria were activated from nutrient slope and grown in nutrient broth at 37°C for 24 h, after which the surfaces of Petri dishes were uniformly inoculated with 0.2 mL of 24 h old test bacteria culture. Using a sterile cork borer, 7 mm wells were bored into the agar and 100 μg/mL solution of each test compound in DMSO was introduced to the well. The plates were thereafter allowed to stand on the bench for 30 min before incubation at 37°C for 24 h, after which the inhibitory zone (in mm) was taken as a measure of their antibacterial activities.

2.4.2. Antifungal Assay (Disc Diffusion Method). A disc application technique was employed *in vitro* to evaluate the antifungal activities of the compounds [37]. The fungi used for the screening were *Aspergillus niger* and *Fusarium oxysporum*. Mature conidia of fungal isolates were harvested from potato dextrose agar (PDA) plates and suspended in ringer solution. Conidial suspension (1 mL) representing each fungal isolate was then spread on a 90 mm Petri dish containing PDA (20 mL) with the excess of the conidial suspension decanted and allowed to dry. The 100 μg/mL compounds were dissolved in dimethyl sulfoxide (DMSO). Sterile 6 mm diameter test discs were impregnated with 15 μL of the solution of each test compound to contain 100 μg/disc in triplicate. Fluconazole (100 μg/disc) was used as a reference drug for fungal inhibition, while DMSO was used as a negative control. Plates were incubated at room temperature for 24 h. The radius of the inhibition zone of fungal growth was measured after 1 day and expressed as the inhibition zone in mm.

2.4.3. Bovine Serum Albumin Denaturation Assay. Bovine serum albumin denaturation assay is used to assess the antidenaturation/anti-inflammatory effect of compounds. The study was done following the method of Mizushima and Kobayashi [38] with slight modification. The standard drug and test compounds were dissolved in DMSO and diluted with phosphate buffer (0.2 M, pH 7.4). Final concentration of DMSO in all solutions was less than 2.5%. Test solution

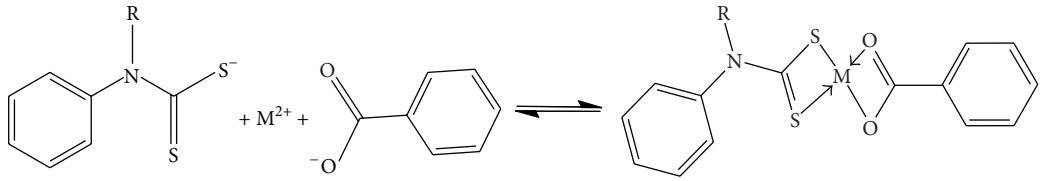

Scheme 1

(1 mL) was mixed (at 50, 100, 200, and 300 μg/mL) with 1 mL of 1 mM albumin solution prepared in phosphate buffer and incubated at 270°C for 10 min. Denaturation was induced by keeping the reaction mixture at 80°C in a water bath for 15 min. After cooling, the turbidity was measured at 660 nm spectrophotometrically. A control was prepared with bovine serum albumin (BSA) in DMSO and was used for the calculation of percentage of inhibition of denaturation [38]. The activity was calculated using the formula

$$\%\ \text{inhibition} = \frac{A_c - A_s}{A_c} \times 100, \tag{4}$$

where A_c is the absorbance of control reaction and A_s is the absorbance of sample.

2.4.4. DPPH Free-Radical Scavenging Assay. 2,2-Diphenyl-1-picrylhydrazyl (DPPH) is a stable free radical that has been widely used as a tool to estimate the free-radical scavenging activity of antioxidants. The reduction capacity of the DPPH radical was determined by the decrease of absorbance induced by antioxidants, according to Brands-williams et al. [39] with a few modifications. The reaction system consisted of 1.1 mL of the test compounds and the standards (acetic acid) diluted to different concentrations (50, 100, 200, and 300 μg/mL) and 2.9 mL of 0.025 g/L DPPH in DMSO. The mixture was shaken vigorously and left to stand (in the dark) at room temperature for 30 min. The absorbance was measured at 517 nm against a blank. The ability to scavenge the DPPH radical was calculated using the following formula:

$$\text{DPPH scavenging effect}\% = \frac{A_o - A_s}{A_o} \times 100; \tag{5}$$

A_o is the absorbance of the control (3 mL of DPPH in DMSO) and A_s is the absorbance of the sample.

2.4.5. Ferrous Chelating Ability Studies. The ferrous ion-chelating ability was determined by the standard colorimetric method [40]. 1 mL of 1,10-phenanthroline (50 mg in 100 mL of DMSO), 1 mL of $FeSO_4 \cdot 7H_2O$ (400 μM), and 1 mL of sample solution of the same concentration (1.0 mg/mL) were mixed together and stirred mechanically for five minutes, while 2 mL of DMSO was added. The resulting homogeneous solution was then incubated at room temperature for 15 min, after which the absorbance of the sample was measured at 546 nm spectrophotometrically. The blank contained 2 mL DMSO, 1 mL 1,10-phenanthroline (50 mg in 100 mL of DMSO), and 1 mL $FeSO_4 \cdot 7H_2O$ (400 μM) solution, respectively. Ascorbic acid was used as the standard [40]. The tests were conducted in triplicate and percentage scavenging inhibition of ferrous ion-chelating ability was also expressed by the following equation:

$$\%\ \text{ferrous chelating ability} = \frac{A_o - A_s}{A_o} \times 100; \tag{6}$$

A_o is the absorbance of the control and A_s is the absorbance of the sample.

3. Results and Discussion

3.1. Synthesis. Treatment of the respective metal salts (nickel(II) chloride hexahydrate and zinc(II) sulphate heptahydrate) with a mixture of benzoic acid and the corresponding dithiocarbamate ligands in ethanol (1 : 1 : 1 ratio) afforded different precipitates of the mixed-ligand complexes. The resulting complexes are colored solids, soluble in DMF and DMSO, and are partially soluble in common organic solvents. They are stable at room temperature, and their geometry was elucidated based on their elemental and spectral studies which were found to be in agreement with the proposed structure of the metal complexes.

3.2. Electronic Absorption Spectra. The ultraviolet bands for the Ni(II) and Zn(II) MDBz mixed-ligand complexes were observed around 46950 ($n \rightarrow \pi^*$) and 29330 ($\pi \rightarrow \pi^*$) cm^{-1} for Zn(II) and 41150 ($n \rightarrow \pi^*$) and 29499 ($\pi \rightarrow \pi^*$) cm^{-1} for Ni(II). The ultraviolet bands for the Ni(II) and Zn(II) in the EDBz series were found around 32790 ($n \rightarrow \pi^*$) and 28650 ($\pi \rightarrow \pi^*$) cm^{-1} for Zn(II) and 40323 ($n \rightarrow \pi^*$) and 29340 ($\pi \rightarrow \pi^*$) cm^{-1} for Ni(II). The ultraviolet bands observed for complexes in the MDBz series were seen to be larger than those found for complexes of EDBz series. This is due to the lower crystal field splitting energy of the molecular orbitals in the MDBz series compared to those of the EDBz series as you move from methyl substitution to ethyl substitution in the dithiocarbamate.

The visible spectra for the zinc complexes of MDBz and EDBz series showed no d-d transitions but metal-to-ligand charge transfer transition at 24940 cm^{-1} for ZnMDB and at 24960 cm^{-1} for ZnEDBz [13, 34]. The visible spectra for the nickel complexes showed d-d transitions that are consistent with square planar geometry [12]. NiMDBz showed bands at 15699 and 18692 cm^{-1} which are assigned to $^1A_{1g} \rightarrow {}^1B_{1g}$ and

$^1A_{1g} \rightarrow {}^1A_{2g}$, respectively. NiEDBz showed visible bands at 15601 and 15015 cm^{-1} which were assigned to $^1A_{1g} \rightarrow {}^1B_{1g}$ and $^1A_{1g} \rightarrow {}^1A_{2g}$ transitions, respectively [12, 33, 34].

3.3. Magnetic and Conductivity Measurements. The magnetic susceptibility measurement was carried out for the metal complexes at room temperature, and the diamagnetic corrections were calculated using Pascal's constant. The ZnEDBz and ZnMDBz complexes were found to be diamagnetic. This is consistent with Zn(II) complexes of d^{10} system which has all the 3d electrons paired [41]. The four coordinate complexes were assigned tetrahedral geometries. The NiEDBz and NiMDBz complexes have moments below zero which has been attributed to distorted square planar geometries. A d^8 system can only exhibit the absence of an unpaired electron (a diamagnetic property) if a square planar geometry has been adopted by the complex; hence, a subzero moment is recorded [42, 43]. A magnetic moment of 2.90–3.30 BM is expected for an octahedral geometry and 3.20–4.10 BM is expected for a tetrahedral geometry for a nickel complex [44, 45]. NiMDBz had a moment of 0.38 BM, while NiEDBz had a magnetic moment of 0.47 BM.

The conductivity measurements were carried out in DMSO at a concentration of 10 mmol and recorded as $\Omega^{-1}cm^2mol^{-1}$. The complexes showed values between 5.16 and 19.9 $\Omega^{-1}cm^2mol^{-1}$. Values below 60 $\Omega^{-1}cm^2mol^{-1}$ are expected for nonelectrolytic complexes, while, for 1 : 1 electrolytes, a value between 60 and 90 $\Omega^{-1}cm^2mol^{-1}$ is expected [46, 47]. Hence, the mixed-ligand complexes are nonelectrolytes.

3.4. Infrared Spectra. The infrared spectra of the complexes were measured from 400 to 4000 cm^{-1}. The stretching vibration bands due to the O-H group of water of crystallization molecules in the complexes appeared between 3478 and 3577 cm^{-1}. The C=O stretching vibration bands of the coordinated carbonyl group of the benzoic acid were observed as sharp bands between 1556 and 1578 cm^{-1} [48], while the C-O stretching vibration bands of the benzoate and the ν(C2-N) peaks of the dithiocarbamate molecules appeared as sharp band around 1287 to 1262 cm^{-1}, respectively. The vibration bands at 2937 and 2792 cm^{-1} are due to the C-H vibration stretching bands of the alkyl groups of the dithiocarbamate ligand, respectively. The ν(C=N) stretching vibration bands of the dithiocarbamate moiety in the complexes appeared as sharp bands between 1483 and 1459 cm^{-1} [49]. The ν(C=S) frequency appeared at 910 cm^{-1} in the spectrum of NiMDBz complex, at 917 cm^{-1} in ZnMDBz and NiEDBz complex, and at 923 cm^{-1} in ZnEDBz complex. The appearance of only one peak in this region indicates symmetrical bonding of the sulphur atoms of the dithiocarbamate ligand to the central metal ion. Stretching bands for ν(M-O) bands from the benzoic acid moiety can be seen around 449–465 cm^{-1}. The ν(M-S) stretching bands for dithiocarbamates usually fall below 400 cm^{-1} and thus could not be observed within the limit of our spectral measurements. Aromatic hydrogen stretching bands, ν(Ar-H), were observed as medium bands between 3004 and 3023 cm^{-1} in the complexes [50].

3.5. Quantum Chemical Calculations. The optimized structures of the studied ligands (MD, ED, and Bz) and their Ni(II) and Zn(II) complexes are displayed alongside their HOMO and LUMO graphics in Figures 1 and 2. Only the atoms referenced in the discussion of the results are numbered in the figures. The HOMOs of all the three ligands are essentially localized on the highly electronegative S and O atoms in their molecules. Slight delocalization towards the aromatic moiety was also observed. The LUMOs of the three ligands, however, are mainly delocalized over the aromatic phenyl ring. The optimized structures of the metal complexes in Figure 2 showed that the central Ni(II) ions in NiMDBz and NiEDBz complexes adopted square planar geometries, while the Zn(II) ions in ZnMDBz and ZnEDBz complexes assumed distorted tetrahedral geometries. The HOMOs of the Ni(II) complexes are principally localized on the S and O atoms as well as the central Ni(II) ions, while the HOMOs of the Zn(II) complexes are only localized on the S atoms. The LUMOs of the Zn(II) complexes are distributed over the entire aromatic ring of the Bz moiety. The change in alkyl chain from $-CH_3$ (in MD) to $-CH_2CH_3$ (in ED) does not have any significant influence on the electron density distribution of the HOMO and LUMO surfaces of the metal complexes.

Selected bond lengths, bond angles, and dihedral angles of the studied ligands and their metals complexes are presented in Table 1. The metal-sulphur (M-S) bond lengths of the complexes reported in Table 1 are in good agreement with what has been reported in the literature for systems containing similar bonds [51, 52], though with different ligands. Similarly, the M-O bond lengths obtained for the studied systems are reasonably within the range of values that have been reported for Ni-O and Zn-O in Ni(II) and Zn(II) complexes of ligands with oxygen coordination sites in the literature [19, 20]. The M-S bond lengths in Table 1 decrease in the order ZnMDBz > ZnEDBz > NiEDBz > NiMDBz, confirming the Ni-S bond to be stronger than Zn-S, which is in agreement with previous studies on comparative strength of Ni-S and Zn-S bonds [18, 19]. Similarly, the decreasing order of M-O bond is ZnEDBz ≈ ZnMDBz > NiEDBz > NiMDBz, also confirming Ni-O bond in the studied systems to be stronger than Zn-O bond. The shorter bond length of Ni-X compared to Zn-X (X = S, O) may be attributed to the shorter ionic radius of Ni(II) ion (0.69 Å) compared to Zn(II) ion (0.74 Å) [53].

Common bonds such as C3-S1, C3-S2, C3-N, and C4-N in MD and ED ligands differ only by ±0.002–0.003 Å, being generally longer in ED. This is due to the slightly better electron-donating ability of ethyl group than of methyl group, which increases the electron density around these bonds in ED as compared to MD. The C5-N bond in the ligands seems to be invariant with the change in alkyl chain. Bonds such as C1-C2, C2-O1, C2-O2, C3-S1, C3-S2, C3-N, C4-N, and C5-N in the ligands appear to be slightly shorter or longer upon complexation with metal ions. This is evidence of redistribution of electron density around these bonds after

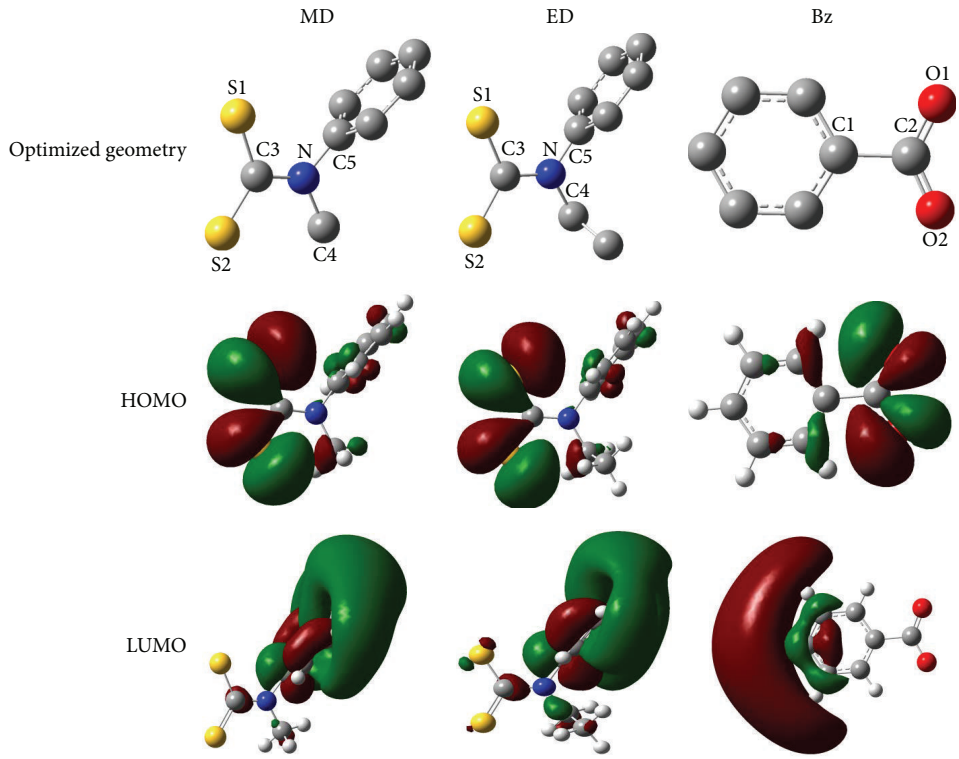

Figure 1: Optimized structures and HOMO and LUMO graphics of MD, ED, and Bz at B3LYP/6-31+G(d,p).

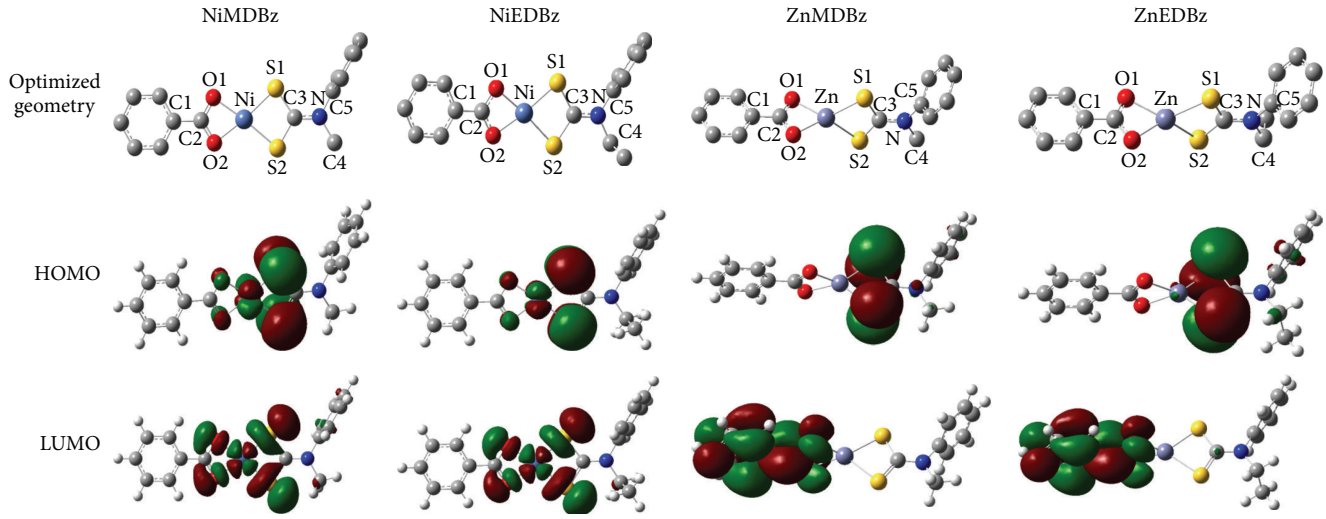

Figure 2: Optimized structures and HOMO and LUMO surfaces of NiMDBz, NiEDBz, ZnMDBz, and ZnEDBz at B3LYP/6-31+G(d,p)/LANL2DZ.

complexation. The bond angles S1-M-S2 and O1-M-O2 are not significantly affected by the change in alkyl substituent on the ligand from $-CH_3$ (MD) to $-CH_2CH_3$ (ED). The dihedral angles around the central metal ions in the studied complexes clearly revealed the planar geometry of Ni(II) ions and distorted tetrahedral geometry of Zn(II) ions in their respective complexes.

Some electronic and thermodynamic parameters were calculated for the metal complexes and the results are presented in Table 2. The frontier molecular orbital energy parameters such as E_{HOMO}, E_{LUMO}, and $\Delta E_{LUMO\text{-}HOMO}$ are often used as reactivity or stability indices. A high value of E_{HOMO} implies better tendency of a molecule to donate its most loosely bound electron to the appropriate orbitals of an acceptor molecule. The decreasing order of E_{HOMO} of the studied metal complexes is NiEDBz > NiMDBz > ZnEDBz > ZnMDBz, which implies that the Ni(II) complex has better tendency to donate its highest energy electron to a suitable

Table 1: Selected geometry parameters: bond lengths (Å), bond angles (°), and dihedral angles (°) of the optimized geometries[a].

Geometry parameter	NiMDBz	NiEDBz	ZnMDBz	ZnEDBz	MD	ED	Bz
Ni-S1/Zn-S1	2.253	2.289	2.456	2.454	—	—	
Ni-S2/Zn-S2	2.256	2.291	2.469	2.466	—	—	
Average Ni-S/Zn-S	2.254	2.290	2.462	2.460	—	—	
Ni-O1/Zn-O1	1.946	1.964	2.093	2.092	—	—	
Ni-O2/Zn-O2	1.952	1.969	2.093	2.094	—	—	
Average Ni-O/Zn-O	1.949	1.966	2.093	2.093	—	—	
C1-C2	1.479	1.463	1.470	1.470	—	—	1.552
C2-O1	1.282	1.310	1.307	1.307	—	—	1.260
C2-O2	1.281	1.309	1.307	1.307	—	—	1.260
C3-S1	1.726	1.778	1.794	1.796	1.719	1.717	—
C3-S2	1.727	1.784	1.794	1.799	1.719	1.722	—
C3-N	1.341	1.338	1.341	1.342	1.395	1.398	—
C4-N	1.471	1.495	1.485	1.497	1.463	1.469	—
C5-N	1.445	1.454	1.456	1.456	1.434	1.434	—
S1-(Ni/Zn)-S2	78.98	80.05	77.78	77.75	—	—	—
O1-(Ni/Zn)-O2	67.87	68.23	64.47	64.47	—	—	—
S1-C3-S2	112.31	111.50	119.00	118.36	125.08	124.39	—
O1-C2-O2	116.20	114.78	117.32	117.32	—	—	129.17
O1-(Ni/Zn)-S1-C3	−179.95	−179.93	−134.13	133.63	—	—	—
O1-(Ni/Zn)-S2-C3	178.11	−178.19	135.75	−135.02	—	—	—
O2-(Ni/Zn)-S1-C3	179.50	179.83	133.96	−135.28	—	—	—
O2-(Ni/Zn)-S2-C3	−179.82	179.77	−135.59	135.52	—	—	—

[a]Ni-X/Zn-X = Ni-X or Zn-X bond accordingly. -(Ni/Zn)- = bond angle or dihedral angle involving Ni or Zn accordingly.

Table 2: Some electronic and thermodynamic parameters of NiMDBz, NiEDBz, ZnMDBz, and ZnEDBz[b].

Parameters	NiMDBz	NiEDBz	ZnMDBz	ZnEDBz
E_{HOMO} (eV)	−6.14	−6.04	−6.39	−6.37
E_{LUMO} (eV)	−2.33	−2.38	−1.41	−1.40
$\Delta E_{LUMO\text{-}HOMO}$ (eV)	3.81	3.66	4.98	4.97
I (eV)	6.14	6.04	6.39	6.37
A (eV)	2.33	2.33	1.41	1.40
χ (eV)	4.24	4.18	3.90	3.88
η (eV)	1.91	1.86	2.50	2.48
μ (Debye)	4.14	4.31	3.66	3.73
BE (kcal/mol)	−687.01	498.58	−402.91	394.52
ΔH (kcal/mol)	−687.40	−499.19	−403.18	−394.76
ΔS (cal/mol)	−68.788	−72.38	−69.46	−68.35
ΔG (kcal/mol)	−666.89	−477.61	−382.47	−374.38

[b]All thermodynamic parameters are zero-point and thermal energies corrected. Thermodynamic data for monatomic M^{2+} (M = Ni, Zn) ions were obtained from B3LYP/LANL2DZ theory.

orbital of an acceptor molecule than its corresponding Zn(II) complex. More so, M-EDBz complexes have better electron-donating ability than M-MDBz complexes. The difference in the values of E_{HOMO} between MDBz and EDBz complexes is more apparent for Ni(II) complexes (±0.1 eV) than Zn(II) complexes (±0.02 eV). The values of E_{LUMO} also revealed that Ni(II) complexes are better electron acceptor than Zn(II) complexes. $\Delta E_{LUMO\text{-}HOMO}$ (energy gap) of the four complexes is in the order ZnMDBz > ZnEDBz > NiMDBz > NiEDBz, predicting the Ni(II) complexes to be more reactive than Zn(II) complexes. The trend of the global hardness, η, is the same as that of energy gap. More so, the more reactive metal complex has higher dipole moment according to the values of μ in Table 2. The MDBz complexes generally exhibit higher electronegativity than the corresponding EDBz complexes as shown by the calculated values of χ. BE, ΔH, and ΔG values showed that the formation of MDBz complexes is more thermodynamically favourable than of the EDBz complexes, and the formation of Ni(II) complexes is more thermodynamically feasible than of Zn(II) complexes. However,

Table 3: A summary of the antimicrobial activities of the mixed-ligand complexes.

Name	Bacteria						Fungi	
	S. aureus	*S. pneumoniae*	*B. subtilis*	*E. coli*	*K. oxytoca*	*P. aeruginosa*	*A. niger*	*F. oxysporum*
[NiMDBz]	16.2 ± 0.4	20.8 ± 0.7	14.2 ± 1.0	17.6 ± 0.4	15.7 ± 0.1	17.8 ± 0.7	17.5 ± 0.1	19.8 ± 0.4
[NiEDBz]	13.8 ± 1.2	8.5 ± 1.1	12.3 ± 0.7	15.0 ± 0	12.4 ± 1.8	11.8 ± 0.7	7.2 ± 0.5	10.5 ± 1.2
[ZnMDBz]	19.0 ± 0.7	20.4 ± 1.0	11.3 ± 0.4	17.4 ± 0.5	19.5 ± 0.3	13.7 ± 0.4	11.2 ± 0	16.4 ± 1.8
[ZnEDBz]	15.7 ± 0.4	17.1 ± 2.1	10.5 ± 1.1	18.6 ± 0.4	11.6 ± 0.1	8.3 ± 0.5	13.5 ± 0.2	7.5 ± 0.4
Streptomycin	23.0 ± 0	25.4 ± 0.3	20.0 ± 0.7	25.6 ± 0	22.3 ± 0.4	27.6 ± 1.8	R	R
Fluconazole	—	—	—	—	—	—	23.5 ± 0.4	27.0 ± 0
DMSO	R	R	R	R	R	R	R	R

Values represent the average of three replications. Streptomycin and fluconazole were used as standard for the antibacterial and antifungal evaluation, respectively. "R" denotes "resistant."

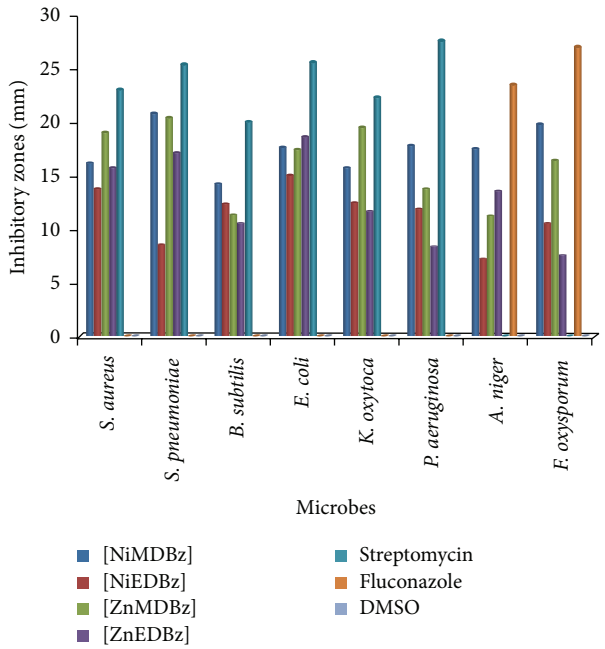

Figure 3: Histogram presentation of the antimicrobial properties of the mixed-ligand complexes.

the formation of NiEDBz is more entropy controlled than NiMDBz. For complexes of the same metal ion, the trends of BE, ΔH, and ΔG are the same as the trends of E_{HOMO} and η. Higher thermodynamic stability of Ni(II) complex in comparison to Zn(II) complex as observed in the present work is in agreement with some previous works [19, 21]. The effect of the relative enhanced electron-donating ability of the ethyl group as compared to the methyl group is generally more apparent in the Ni(II) than in Zn(II) complexes.

3.6. Antimicrobial Screening. The growth of inhibition zones after incubation is presented in Table 3 and summarized as histogram in Figure 3. The metal complexes exhibited moderate to high activity against six strains of bacteria and two fungi organisms at a concentration of 100 μg/mL. The complexes were active against all the microbes and in some cases were as active as the control drugs. The NiMDBz and ZnMDBz complexes showed 82% and 80% activity, respectively, when compared to the activity of streptomycin against *S. pneumoniae*. Overall, NiMDBz mixed-ligand complex exhibited the best antimicrobial character among the test compounds against several organisms used for this study. On the basis of ligand structures, the mixed-ligand complexes involving the *N*-methyl-*N*-phenyl dithiocarbamate and benzoate showed better antimicrobial activity compared to those of *N*-ethyl-*N*-phenyl dithiocarbamate and benzoate.

Finally, the antimicrobial activity of the mixed-ligand complexes may be attributed to the fact that dithiocarbamates and benzoates are known to possess antimicrobial property; hence, their structural combination gave rise to heteroleptic metal complexes with improved antimicrobial character. Also, the presence of metal ions in the compound increased toxicity of the ligands towards the microbes [54–57].

The variation in the effectiveness of different compounds against different organisms depends either on the impermeability of the cells of the microbes or on differences in ribosome of microbial cells [58]. Although the exact mechanism is not fully understood biochemically, the mode of action of antimicrobials may involve various targets in microorganisms. The following mechanisms have been suggested: (i) Interference with the cell wall synthesis causes damage, as a result of which cell permeability may be altered or it may disorganize the lipoprotein leading to the cell death; (ii) deactivation of various cellular enzymes, which play a vital role in different metabolic pathways of these microorganisms; (iii) denaturation of one or more proteins of the cell, as a result of which the normal cellular processes are impaired; (iv) formation of a hydrogen bond through the azomethine group with the active center of cell constituents, resulting in interference with the normal cell process [59].

3.7. Anti-Inflammatory Studies. The results of denaturation studies presented in Table 4 showed that the complexes exhibited antidenaturation properties for thermal induced bovine serum albumin. Interestingly, the ability of compounds to inhibit denaturation reduces with increase in concentration. This is considered an advantage because, at higher concentrations, the toxicity of compounds to human cells

Table 4: Antidenaturation (anti-inflammatory activities) results.

Samples	Concentration (μg/mL)	% inhibition	Mean ± SD
Control	—	—	0.0301 ± 0.001
Diclofenac sodium	100	83.39	0.0050 ± 0.001
	200	73.75	0.0079 ± 0.001
	500	67.44	0.0098 ± 0.001
ZnEDBz	100	67.59	0.0098 ± 0.0005
	200	60.13	0.0120 ± 0.001
	500	59.80	0.0121 ± 0.002
NiEDBz	100	72.43	0.0083 ± 0.0005
	200	68.11	0.0096 ± 0.002
	300	62.21	0.0114 ± 0.0005
ZnMDBz	100	43.19	0.0171 ± 0.001
	200	41.86	0.0175 ± 0.0005
	500	39.20	0.0183 ± 0.0005
NiMDBz	100	57.81	0.0127 ± 0.001
	200	54.15	0.0138 ± 0.001
	500	49.37	0.0152 ± 0.0005

increases. Therefore, at lower concentration, the compounds can effectively inhibit thermal denaturation of albumin with low toxicity.

NiEDBz was found to have the highest percentage inhibition of 72.43% of all the test compounds while ZnMDBz showed the lowest inhibition property of 39.20%. However, the EDBz complexes had the highest anti-inflammatory property but not greater than that of diclofenac sodium that was used as the control drug.

3.8. Antioxidant Studies

3.8.1. DPPH. DPPH is a stable free radical containing an odd electron in its structure and usually used for the detection of the radical scavenging activity in chemical analysis [60]. The model of scavenging the stable DPPH$^{\bullet}$ radical is a widely used method to evaluate antioxidant activities in a relatively short time compared with other methods. The maximum absorption of a stable DPPH$^{\bullet}$ radical in DMSO was at 517 nm. When there is a reaction between antioxidant molecules and DPPH$^{\bullet}$ radical, it results in the scavenging of the radical by hydrogen or electron donation, which causes a decrease of the absorbance of DPPH$^{\bullet}$ radical. This is visually noticeable as discoloration from purple to yellow. Hence, DPPH$^{\bullet}$ is usually used as a substrate to evaluate antioxidant activity of antioxidants [54]. The effect of antioxidants on DPPH$^{\bullet}$ radical scavenging was thought to be due to their hydrogen or electron-donating ability. DPPH$^{\bullet}$ is a stable free radical and accepts an electron or hydrogen radical to become a stable diamagnetic molecule [61]. The scavenging ability of the metal complexes was compared with ascorbic acid as a standard and presented in Figure 4. The metal complexes showed good activities as a radical scavenger compared with ascorbic acid. The Ni complexes showed better antioxidant properties compared to the Zn complexes. However, a better antioxidant property was observed in the ethyl substituted dithiocarbamate complexes overall.

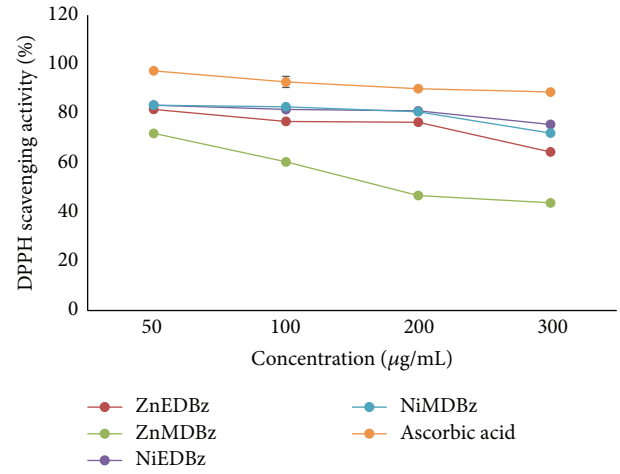

Figure 4: Graph representing DPPH radical scavenging ability of the compounds.

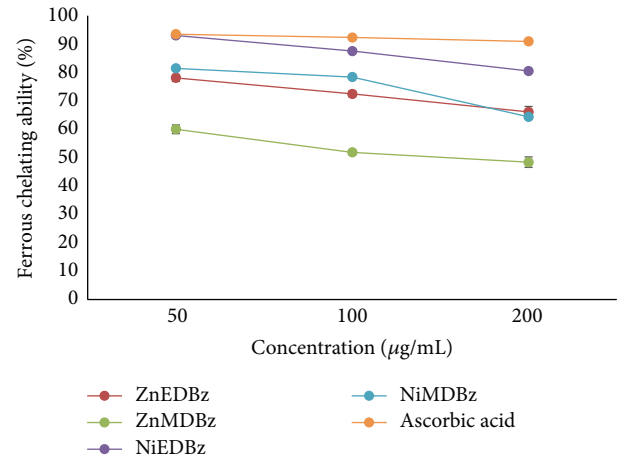

Figure 5: Graph representing % ferrous chelating ability of the compounds.

3.8.2. Ferrous Chelating. Metal chelation is an example of a complexation reaction. 1,10-Phenanthroline was used as complex forming agent of Fe(II) and forms a red coloured Fe(II)-1,10 Phen complex with maximum absorbance at 546 nm. Hence, in the presence of a reducing agent, the complex formation is hampered resulting in the decrease in the colour of the complex and a decrease in the absorbance. Measurement of absorbance therefore allows estimation of the metal chelating activity of the coexisting chelator. The prooxidant metal chelation is one of the most important mechanisms of secondary antioxidants' action. Chelation of metals by certain compounds decreases their prooxidant effect by reducing their redox potentials and stabilizing the oxidized form of the metal [62]. Figure 5 shows the chelating ability of the complexes and ascorbic acid as a concentration-dependent property. The chelating activity order of

the compounds from maximum to minimum was found to be NiEDBz > NiMDBz > ZnEDBz > ZnMDBz at concentrations of 50, 100, and 200 μg/mL. The nickel compounds had better chelating properties compared to the zinc complexes.

4. Conclusions

Some heteroleptic metal complexes of Zn(II) and Ni(II) have been synthesized and characterized. The complexes are four coordinate geometries by bonding to the sulphur atoms of the dithiocarbamate and oxygen atoms of benzoic acid. The electronic spectral and magnetic moment data is in favour of square planar geometry for Ni(II) complexes and tetrahedral geometry for Zn(II) complexes. The covalent nature of the complexes was determined by their conductance measurement. The synthesized compounds showed antibacterial/antifungal properties. In comparison, the *N*-methyl-*N*-phenyl dithiocarbamate and benzoate showed better antimicrobial activity compared to those of *N*-ethyl-*N*-phenyl dithiocarbamate and benzoate, thus introducing a novel class of metal-based bactericidal and fungicidal agents. The complexes also showed anti-inflammatory activity by their ability to inhibit thermal denaturation of bovine serum albumin. The antioxidant potentials of the complexes were investigated using DPPH assay and ferrous chelating assay. The complexes showed good antioxidant properties at a concentration of 50–200 μg/mL. The proposed geometries of the complexes were confirmed to correspond to stable ground state configurations by using the DFT calculations. The theoretically predicted order of reactivity of the complexes using some electronic reactivity indices coincides with some of the experimentally observed trends of biological activity.

Competing Interests

The authors declare that they have no competing interests.

References

[1] Y. Aydogdu, F. Yakuphanoglu, A. Aydogdu, E. Tas, and A. Cukurovali, "Solid state electrical conductivity properties of copper complexes of novel oxime compounds containing oxolane ring," *Materials Letters*, vol. 57, no. 24-25, pp. 3755–3760, 2003.

[2] H.-Y. Bie, J.-H. Yu, Q.-J. Xu et al., "Synthesis, structure and non-linear optical property of a copper(II) thiocyanate three-dimensional supramolecular compound," *Journal of Molecular Structure*, vol. 660, no. 1–3, pp. 107–112, 2003.

[3] X. Xu, T. Xu, J. Gao et al., "Synthesis, crystal structure and properties of a new mixed ligand copper(II) complex [Cu(imH) (aepa)]$(ClO_4)_2$ (imH=imidazole, aepa=N–(2–aminoethyl)–1,3–propylamine)]," *Synthesis and Reactivity in Inorganic Metal-Organic and Nano-Metal Chemistry*, vol. 36, no. 9, pp. 681–686, 2006.

[4] A. R. Sarkar and S. Mandal, "Mixed-ligand peroxo complexes of vanadium containing 2-thiouracil and its 6-methyl derivative," *Synthesis and Reactivity in Inorganic and Metal-Organic Chemistry*, vol. 30, pp. 1477–1488, 2000.

[5] A. A. El-Sherif and B. J. A. Jeragh, "Mixed ligand complexes of Cu(II)-2-(2-pyridyl)-benzimidazole and aliphatic or aromatic dicarboxylic acids: synthesis, characterization and biological activity," *Spectrochimica Acta A*, vol. 68, no. 3, pp. 877–882, 2007.

[6] R. A. Rane, M. Nandave, S. Nayak et al., "Synthesis and pharmacological evaluation of marine bromopyrrole alkaloid-based hybrids with anti-inflammatory activity," *Arabian Journal of Chemistry*, 2014.

[7] K. M. Khan, N. Ambreen, U. R. Mughal, S. Jalil, S. Perveen, and M. I. Choudhary, "3-Formylchromones: potential antiinflammatory agents," *European Journal of Medicinal Chemistry*, vol. 45, no. 9, pp. 4058–4064, 2010.

[8] N. Deattu, N. Narayanan, and L. Suseela, "Evaluation of anti-inflammatory and antioxidant activities of polyherbal extract by in vitro methods," *Research Journal of Pharmaceutical, Biological and Chemical Sciences*, vol. 3, no. 4, pp. 727–732, 2012.

[9] B. K. Manjunatha, S. Murthuza, R. Divakara et al., "Antioxidant and anti-inflammatory potency of mesua ferrea linn," *Indian Journal of Applied Research*, vol. 3, no. 8, pp. 55–59, 2013.

[10] N. H. Grant, H. E. Alburn, and C. Kryzanauskas, "Stabilization of serum albumin by anti-inflammatory drugs," *Biochemical Pharmacology*, vol. 19, no. 3, pp. 715–722, 1970.

[11] E. Middleton Jr., C. Kandaswami, and T. C. Theoharides, "The effects of plant flavonoids on mammalian cells: implications for inflammation, heart disease, and cancer," *Pharmacological Reviews*, vol. 52, no. 4, pp. 673–751, 2000.

[12] S. M. Mamba, A. K. Mishra, B. B. Mamba, P. B. Njobeh, M. F. Dutton, and E. Fosso-Kankeu, "Spectral, thermal and in vitro antimicrobial studies of cyclohexylamine-*N*-dithiocarbamate transition metal complexes," *Spectrochimica Acta Part A: Molecular and Biomolecular Spectroscopy*, vol. 77, no. 3, pp. 579–587, 2010.

[13] H. A. Tajmir-Riahi, M. Langlais, and R. Savoie, "A laser raman spectroscopic study of the interaction of calf-thymus DNA with Cu(II) and Pb(II) ions: metal ion binding and DNA conformational changes," *Nucleic Acids Research*, vol. 16, no. 2, pp. 751–762, 1988.

[14] C. Orvig and M. J. Abrams, "Medicinal inorganic chemistry: introduction," *Chemical Reviews*, vol. 99, no. 9, pp. 2201–2204, 1999.

[15] D. C. Onwudiwe and P. A. Ajibade, "Synthesis and crystal structure of Bis(*N*-alkyl-*N*-phenyl dithiocarbamato)mercury(II)," *Journal of Chemical Crystallography*, vol. 41, no. 7, pp. 980–985, 2011.

[16] A. D. Becke, "Density-functional exchange-energy approximation with correct asymptotic behavior," *Physical Review A*, vol. 38, no. 6, pp. 3098–3100, 1988.

[17] C. Lee, W. Yang, and R. G. Parr, "Development of the Colle-Salvetti correlation-energy formula into a functional of the electron density," *Physical Review B*, vol. 37, no. 2, pp. 785–789, 1988.

[18] I. Georgieva and N. Trendafilova, "Bonding analyses, formation energies, and vibrational properties of M-R2dtc complexes (M = Ag(I), Ni(II), Cu(II), or Zn(II))," *Journal of Physical Chemistry A*, vol. 111, no. 50, pp. 13075–13087, 2007.

[19] Y. Niu, S. Feng, Y. Ding, R. Qu, D. Wang, and J. Han, "Theoretical investigation on sulfur-containing chelating resin-divalent metal complexes," *International Journal of Quantum Chemistry*, vol. 110, no. 10, pp. 1982–1993, 2010.

[20] S. I. Gorelsky, L. Basumallick, J. Vura-Weis et al., "Spectroscopic and DFT investigation of [MHB(3,5-iPr 2pz)3(SC6F5)] (M = Mn, Fe, Co, Ni, Cu, and Zn) model complexes: periodic trends in metal-thiolate bonding," *Inorganic Chemistry*, vol. 44, no. 14, pp. 4947–4960, 2005.

[21] M. J. Frisch, G. W. Trucks, H. B. Schlegel et al., *Gaussian 09, Revision D.01*, Gaussian, Inc., Wallingford, Conn, USA, 2009.

[22] L. Chen, T. Liu, and C. Ma, "Metal complexation and biodegradation of EDTA and S,S-EDDS: a density functional theory study," *The Journal of Physical Chemistry A*, vol. 114, no. 1, pp. 443–454, 2010.

[23] M. Belcastro, T. Marino, N. Russo, and M. Toscano, "Interaction of cysteine with Cu^{2+} and Group IIb (Zn^{2+}, Cd^{2+}, Hg^{2+}) metal cations: a theoretical study," *Journal of Mass Spectrometry*, vol. 40, no. 3, pp. 300–306, 2005.

[24] T. Marino, M. Toscano, N. Russo, and A. Grand, "Structural and electronic characterization of the complexes obtained by the interaction between bare and hydrated first-row transition-metal ions (Mn^{2+}, Fe^{2+}, Co^{2+}, Ni^{2+}, Cu^{2+}, Zn^{2+}) and glycine," *The Journal of Physical Chemistry B*, vol. 110, no. 48, pp. 24666–24673, 2006.

[25] R. Terreux, M. Domard, C. Viton, and A. Domard, "Interactions study between the copper II ion and constitutive elements of chitosan structure by DFT calculation," *Biomacromolecules*, vol. 7, no. 1, pp. 31–37, 2006.

[26] J. C. Amicangelo, "Theoretical characterization of a tridentate photochromic Pt(II) complex using density functional theory methods," *Journal of Chemical Theory and Computation*, vol. 3, no. 6, pp. 2198–2209, 2007.

[27] F. Tarazona-Vasquez and P. B. Balbuena, "Dendrimer-tetrachloroplatinate precursor interactions. 1. Hydration of Pt(II) species and PAMAM outer pockets," *Journal of Physical Chemistry A*, vol. 111, no. 5, pp. 932–944, 2007.

[28] F. Tarazona-Vasquez and P. B. Balbuena, "Dendrimer-tetrachloroplatinate precursor interactions. 2. Noncovalent binding in PAMAM outer pockets," *Journal of Physical Chemistry A*, vol. 111, no. 5, pp. 945–953, 2007.

[29] T. H. Dunning and P. J. Hay, "Gaussian basis sets for molecular calculations," in *Methods of Electronic Structure Theory*, H. F. Schaefer III, Ed., vol. 3 of *Modern Theoretical Chemistry*, Plenum Press, New York, NY, USA, 1977.

[30] P. J. Hay and W. R. Wadt, "Ab initio effective core potentials for molecular calculations. Potentials for the transition metal atoms Sc to Hg," *The Journal of Chemical Physics*, vol. 82, no. 1, pp. 270–283, 1985.

[31] W. R. Wadt and P. J. Hay, "Ab initio effective core potentials for molecular calculations. Potentials for main group elements Na to Bi," *The Journal of Chemical Physics*, vol. 82, no. 1, pp. 284–298, 1985.

[32] P. J. Hay and W. R. Wadt, "Ab initio effective core potentials for molecular calculations. Potentials for K to Au including the outermost core orbitals," *The Journal of Chemical Physics*, vol. 82, no. 1, pp. 299–310, 1985.

[33] J. Sabolović, C. S. Tautermann, T. Loerting, and K. R. Liedl, "Modeling anhydrous and aqua copper(II) amino acid complexes: a new molecular mechanics force field parametrization based on quantum chemical studies and experimental crystal data," *Inorganic Chemistry*, vol. 42, no. 7, pp. 2268–2279, 2003.

[34] M. Y. Combariza and R. W. Vachet, "Effect of coordination geometry on the gas-phase reactivity of four-coordinate divalent metal ion complexes," *The Journal of Physical Chemistry A*, vol. 108, no. 10, pp. 1757–1763, 2004.

[35] M. A. Carvajal, J. J. Novoa, and S. Alvarez, "Choice of coordination number in d^{10} complexes of group 11 metals," *Journal of the American Chemical Society*, vol. 126, no. 5, pp. 1465–1477, 2004.

[36] B. D. Alexander and T. J. Dines, "Ab initio calculations of the structures and vibrational spectra of ethene complexes," *Journal of Physical Chemistry A*, vol. 108, no. 1, pp. 146–156, 2004.

[37] A. C. Ekennia, D. C. Onwudiwe, C. Ume, and E. E. Ebenso, "Mixed ligand complexes of *N*-methyl-*N*-phenyl dithiocarbamate: synthesis, characterisation, antifungal activity, and solvent extraction studies of the ligand," *Bioinorganic Chemistry and Applications*, vol. 2015, Article ID 913424, 10 pages, 2015.

[38] Y. Mizushima and M. Kobayashi, "Interaction of anti-inflammatory drugs with serum proteins, especially with some biologically active proteins," *Journal of Pharmacy and Pharmacology*, vol. 20, no. 3, pp. 169–173, 1968.

[39] W. Brands-Williams, M. E. Cuvelier, and C. Berset, "Use of a free radical method to evaluate antioxidant activity," *Lebensmittel-Wissenschaft & Technologie*, vol. 18, pp. 25–30, 1995.

[40] A. A. Osowole, S. M. Wakil, and M. O. Emmanuel, "Synthesis, characterization, antioxidant and antimicrobial activities of some Metal(II) Complexes of the Mixed-Ligands, Vitamin B_2 and Benzoic acid," *Elixir Applied Chemistry*, vol. 79, pp. 30370–30374, 2015.

[41] L. A. Saghatforoush, A. Aminkhani, S. Ershad, G. Karimnezhad, S. Ghammamy, and R. Kabiri, "Preparation of zinc (II) and cadmium (II) complexes of the tetradentate Schiff base ligand 2-((E)-(2-(2-(pyridine-2-yl)-ethylthio)ethylimino)methyl)-4-bromophenol (PytBrsalH)," *Molecules*, vol. 13, no. 4, pp. 804–811, 2008.

[42] N. Raman, V. Muthuraj, S. Ravichandran, and A. Kulandaisamy, "Synthesis, characterisation and electrochemical behaviour of Cu(II), Co(II), Ni(II) and Zn(II) complexes derived from acetylacetone andp-anisidine and their antimicrobial activity," *Journal of Chemical Sciences*, vol. 115, no. 3, pp. 161–167, 2003.

[43] S. Konstantinovi, B. Radovanovi, I. Caki, and J. Vesnavasi, "Synthesis and characterization of Co(II), Ni(II), Cu(II) and Zn(II) complexes with 3-salicylidenehydrazono-2-indolinone," *Journal of the Serbian Chemical Society*, vol. 68, no. 8-9, pp. 641–647, 2003.

[44] A. A. Osowole, "Studies on some VO(IV), Ni(II) and Cu(II) complexes of non-symmetrical tetradentate Schiff-bases," *Bulletin of the Chemical Society of Ethiopia*, vol. 22, no. 2, pp. 219–224, 2008.

[45] K. Serbest, H. Kayi, M. Er, K. Sancak, and I. Değirmencioğlu, "Ni(II), Cu(II), and Zn(II) complexes of tetradentate schiff base containing two thiadiazoles units: structural, spectroscopic, magnetic properties, and molecular modeling studies," *Heteroatom Chemistry*, vol. 19, no. 7, pp. 700–712, 2008.

[46] I. S. Raja, M. Christudhas, and G. A. G. Raj, "Synthesis, characterization, metal ion intake and antibacterial activity of cardanol based polymeric Schiff base transition metal complexes using Ethylenediamine," *Journal of Chemical and Pharmaceutical Research*, vol. 3, pp. 127–135, 2011.

[47] J. Liu, B. Wu, B. Zhang, and Y. Liu, "Synthesis and characterization of metal complexes of Cu(II), Ni(II), Zn(II), Co(II), Mn(II) and Cd(II) with tetradentate schiff bases," *Turkish Journal of Chemistry*, vol. 30, pp. 41–48, 2006.

[48] N. Dodoff, K. Grancharov, R. Gugova, and N. Spassovska, "Platinum (II) complexes of benzoic- and 3-methoxybenzoic acid hydrazides. Synthesis, characterization, and cytotoxic effect," *Journal of Inorganic Biochemistry*, vol. 54, no. 3, pp. 221–233, 1994.

[49] D. C. Onwudiwe and P. A. Ajibade, "Synthesis, characterization and thermal studies of Zn(II), Cd(II) and Hg(II) complexes of *N*-methyl-*N*-phenyldithiocarbamate: the single

crystal structure of $[(C_6H_5)(CH_3)NCS_2]_4Hg_2$," *International Journal of Molecular Sciences*, vol. 12, no. 3, pp. 1964–1978, 2011.

[50] R. R. Scharfe, V. S. Sastri, and C. L. Chakrabarti, "Stability of metal dithiocarbamate complexes," *Analytical Chemistry*, vol. 45, no. 2, pp. 413–415, 1973.

[51] J. Zhang, A. Adhikary, K. M. King, J. A. Krause, and H. Guan, "Substituent effects on Ni–S bond dissociation energies and kinetic stability of nickel arylthiolate complexes supported by a bis(phosphinite)-based pincer ligand," *Dalton Transactions*, vol. 41, no. 26, pp. 7959–7968, 2012.

[52] T. Sakajiri, H. Yajima, and T. Yamamura, "Density functional theory study on metal-binding energies for human serum transferrin-metal complexes," *ISRN Biophysics*, vol. 2012, Article ID 124803, 5 pages, 2012.

[53] H. Sun, H. Li, and P. J. Sadler, "Transferrin as a metal ion mediator," *Chemical Reviews*, vol. 99, no. 9, pp. 2817–2842, 1999.

[54] J. R. Soares, T. C. P. Dinis, A. P. Cunha, and L. M. Almeida, "Antioxidant activities of some extracts of Thymus zygis," *Free Radical Research*, vol. 26, no. 5, pp. 469–478, 1997.

[55] L. Mishra and V. K. Singh, "Synthesis and structural and antifungal studies of Co(II), Ni(II), Cu(II) and Zn(II) complexes with new Schiff bases bearing benzimidazoles," *Indian Journal of Chemistry A*, vol. 32, pp. 446–449, 2007.

[56] N. H. Al-Shaalan, "Synthesis, characterization and biological activities of Cu(II), Co(II), Mn(II), Fe(II), and UO 2(VI) complexes with a new Schiff base hydrazone: O-hydroxyacetophenone-7-chloro-4-quinoline hydrazone," *Molecules*, vol. 16, no. 10, pp. 8629–8645, 2011.

[57] T. Arunachalam, R. Bhakyaraj, and A. K. Sasi, "Synthesis, characterization and biological activity of Mn^{2+}, Co^{2+}, Ni^{2+} and Cu^{2+} complexes of benzoic acid ligand," *E-Journal of Chemistry*, vol. 6, no. 3, pp. 743–746, 2009.

[58] R. S. Joseyphus and M. S. Nair, "Antibacterial and antifungal studies on some Schiff base complexes of Zinc(II)," *Mycobiology*, vol. 36, no. 2, pp. 93–98, 2008.

[59] L. Malhota, S. Kumar, and K. S. Dhindsa, "Synthesis, characterization and microbial activity of Co(II), Ni(II), Cu(II) and Zn(II) complexes of aryloxyacetic acid and hydrazides," *Indian Journal of Chemistry Section A*, vol. 32, pp. 457–459, 1993.

[60] S. Nithiya, N. Karthik, and J. Jayabharathi, "In vitro antioxidant activity of hindered piperidone derivatives," *International Journal of Pharmacy and Pharmaceutical Sciences*, vol. 3, no. 3, pp. 254–256, 2011.

[61] Z. I. Fatimah, Z. Zaiton, M. Jamaludin, M. T. Gapor, M. I. Nafeeza, and O. Khairul, "Effect of estrogen and palm vitamin E on malondialdehyde levels toward the development of arteriosclerosis in the New Zealand white rabbit," in *Biological Oxidants and Antioxidants: Molecular Mechanism and Health Effects*, L. Packer and S. H. Ong, Eds., AOCS Press, Champaign, Ill, USA, 1998.

[62] D. W. Reische, D. A. Lillard, and R. R. Eitenmiller, "Antioxidants," in *Food Lipids Chemistry Nutrition, and Biotechnology*, C. C. Akoh and D. B. Min, Eds., pp. 409–433, CRC Press, New York, NY, USA, 3rd edition, 2008.